# Hydrogel Interferometry for Ultrasensitive and Highly Selective Chemical Detection

*Mo Sun, Ruobing Bai, Xingyun Yang, Jiaqi Song, Meng Qin, Zhigang Suo, and Ximin He\**

Developing ultrasensitive chemical sensors with small scale and fast response through simple design and low-cost fabrication is highly desired but still challenging. Herein, a simple and universal sensing platform based on a hydrogel interferometer with femtomol-level sensitivity in detecting (bio)chemical molecules is demonstrated. A unique local concentrating effect (up to $10^9$ folds) in the hydrogel induced by the strong analyte binding and large amount of ligands, combined with the signal amplification effect by optical interference, endows this platform with an ultrahigh sensitivity, specifically $10^{-14}$ M for copper ions and $1.0 \times 10^{-11}$ mg mL$^{-1}$ for glycoprotein with 2–4 order-of-magnitude enhancement. The specific chemical reactions between selected ligands and target analytes provide high selectivity in detecting complex fluids. This universal principle with broad chemistry, simple physics, and modular design allows for high performance in detecting wide customer choices of analytes, including metal ions and proteins. The scale of the sensor can be down to micrometer size. The nature of the soft gel makes this platform transparent, flexible, stretchable, and compatible with a variety of substrates, showing high sensing stability and robustness after 200 cycles of bending or stretching. The outstanding sensing performance grants this platform great promise in broad practical applications.

With an ever high demand of real-time health and environment monitoring and prevalent smart technologies nowadays, high-precision molecule detection with micro-sized devices is playing a vital role with many exciting progresses recently.[1] Ultrasensitivity is critical for detecting trace-amount analyte, which is vital for healthcare, ecology, and industries.[2] For example,

Dr. M. Sun, X. Yang, J. Song, Dr. M. Qin, Prof. X. He
Department of Materials Science and Engineering
University of California
Los Angeles, CA 90095, USA
E-mail: ximinhe@ucla.edu
Dr. R. Bai, Prof. Z. Suo
John A. Paulson School of Engineering and Applied Sciences
Kavli Institute for Bionano Science and Technology
Harvard University
Cambridge, MA 02138, USA
Prof. X. He
California Nanosystems Institute
Los Angeles, CA 90095, USA

The ORCID identification number(s) for the author(s) of this article can be found under https://doi.org/10.1002/adma.201804916.

free copper ions in ocean should be critically maintained between picoM and femtoM ($10^{-12}$ and $10^{-15}$ M) to be micronutrients for organisms, which would become toxic at a higher concentration.[3] Hence, accurately mapping and real-time monitoring copper distribution are important for marine biological recycling and scavenging. Wilson's disease, a hepatic and neurological disorder, is diagnosed of the 24 h urinary copper excretion (>100 µg/24 h).[4] On-site fast detection of the trace-amount copper ions with personal metabolism monitoring devices could effectively prevent or reverse many manifestations of this disorder.[5] However, current methods of detecting such low amounts of metal ions still rely on complex and costly analyte preconcentrating or presorting, as well as large instrument operated by well-trained laboratory personnel, such as inductively coupled plasma mass spectroscopy (ICP-MS) and atomic absorption/emission spectroscopy (AAS/AES).[6] Thus, real-time monitoring industry or sea water cannot be achieved by these methods. Similarly, detecting specific proteins nowadays typically uses western blot or enzyme-linked immunosorbent assay (ELISA), both of which involve lengthy multistep processes of proteins enrichment, staining, and detection. These detection methods can reach desired low limit of detection (LOD), but their large equipment size and high cost prevent them from facilitating personal healthcare or point-of-care technologies.[7] There have been great research efforts on advancing microscale sensors for detecting metal ions and biomolecules (e.g., protein and enzyme); however, the state-of-the-art sensitivity of, for example, copper ion detection is $10^{-4}$–$10^{-10}$ M,[5b,6,8] and that of horse radish protease detection is $10^{-4}$–$10^{-7}$ M,[9] which still have not reached the aforementioned desired sensitivity levels. As a long-sought solution to above issues, creating small-scale synthetic chemical sensors with high sensitivity and high selectivity is proven a daunting challenge, due to the time-consuming and still expensive synthesis, purification, and manufacturing processes.[10]

We have recently described hydrogel interferometry as a low-cost, general-purpose platform for chemical detection.[11] Here we show that hydrogel interferometry can achieve chemical detection of exceptionally high sensitivity and selectivity
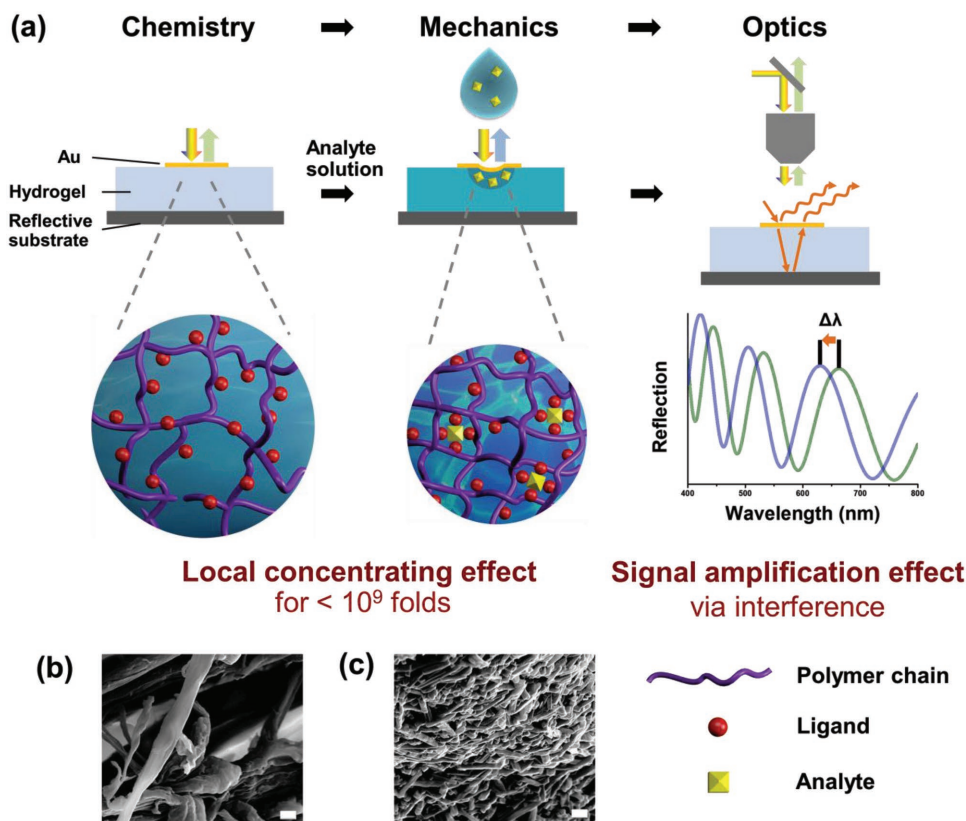
**ADVANCED
SCIENCE NEWS**
www.advancedsciencenews.com

**ADVANCED
MATERIALS**
www.advmat.de

**Figure 1.** a) Sensing mechanism of the hydrogel interferometer platform: the complete chemical-mechanical-optical signal transduction process. b,c) The SEM images of hydrogel before (b) and after (c) adding $Cu^{2+}$ ions into it. The scale bar is 1 µm.

through the synergy of chemistry, mechanics, and optics. A hydrogel interferometer consists of a reflective substrate coated with a single thin film of hydrogel (**Figure 1**). Hydrogel as a highly porous cross-linked polymer network is chosen for its unique large volume change ratio up to ≈10 times, chemical functionalization for broad stimuli sensitivities, and mechanical flexibility.[12] The polymer network of the hydrogel provides a scaffold to carry a large number of ligands specific to the analyte (ligand-to-polymer mass ratio = 1:5). The thickness of the hydrogel is comparable to the wavelength of visible light (≈300 nm at dry state and ≈1000 nm at hydrated state). When a drop of analyte-containing solution is applied on the surface of the hydrogel, the analyte diffuses into the hydrogel, causing a cascade of signal transduction, involving chemical reaction, mechanical deformation, and optical detection (C→M→O). The ligands capture and localize the analyte by forming complexes. Such a strong and local ligand-analyte binding effectively concentrates the analyte within an extremely small volume of the gel for as high as $10^9$ folds (i.e., concentrating an analyte droplet of 10 µL or $1 \times 10^{10}$ µm$^3$ into a 1.7 µm$^3$ volume). Compared to other high-performance sensors based on rigid porous carrier such as metal–organic framework,[13] the unique large volumetric shrinkage (≈10%) of the soft gel network further enhances the magnitude of this local concentrating effect. As a result of the ligand-analyte binding, the gel locally contracts or swells, depending on the ligand-to-analyte ratio, which leads to local thickness change. A thickness change

as small as a few nanometers can be detected through optical interference, known as a significant signal amplifier. Overall, the two key merits, the analyte concentrating effect (in C→M) and the subsequent signal amplification (in M→O) jointly lead to the remarkably low LOD at an unprecedented level while possessing great selectivity. Specifically, we achieved LODs of $10^{-14}$ M in $Cu^{2+}$ detection and $10^{-11}$ mg mL$^{-1}$ in glycoprotein detection against multiple interfering species in mixture analyte fluids, which present 2–4 order-of-magnitude enhancements in sensitivity over the state-of-the-art methods in analyzing real-life complex fluids. Moreover, achieving such high sensitivity and selectivity requires only a micrometer-sized hydrogel. In addition, such hydrogel interferometer can be constructed into transparent and flexible sensors with various substrates. This simple but general platform with a single layer of hydrogel can accommodates broad choices of ligands and substrates. Therefore, it can be readily customized for detecting many chemical and biological species in the fields from healthcare to environment safety and integrated to wearable electronics. Overall, this unique hydrogel interferometer-based sensing platform adopts a highly efficient chemo-mechano-optical signal transduction that enables fM-level sensitivity on a sub-µm$^3$ sensing active region. In combination with the great selectivity, optical transparency, and mechanical flexibility, it presents promise for the next-generation high-performance micro-sensors.

We first prove this concept by creating a high-sensitivity $Cu^{2+}$ sensor. Imidazole can bind with $Cu^{2+}$ ions specifically

to form complexes in aqueous solutions.[14] By grafting imidazole ligands on the polymer chains of a hydrogel, the hydrogel becomes $Cu^{2+}$-sensitive. When a droplet of $Cu^{2+}$ analyte aqueous solution is applied onto such an imidazole-rich hydrogel, the $Cu^{2+}$ ions diffuse in and bind with the imidazole ligands on the polymer chains. Because the binding constant between $Cu^{2+}$ and imidazole is fairly high,[14] and the concentration of imidazole is much higher than that of $Cu^{2+}$, these favor for the right-shifting of the coordination reaction, facilitating the formation of the $Cu^{2+}$–imidazole complexes. In the case of detecting $Cu^{2+}$ at low concentrations with the large amount ligands in the hydrogel, the $Cu^{2+}$–imidazole complexes form at a 1:4 ratio. Hence, each $Cu^{2+}$ ion bring the multiple surrounding polymer chains together, the complexes serve as additional crosslinks of the hydrogel, and as a result, the hydrogel swelling ratio decreases with the concentration of $Cu^{2+}$ in the analyte solution. As the SEM images in Figure 1b,c show, after adding $Cu^{2+}$ into the hydrogel, the hydrogel pore size significantly reduced and the gel network became much denser. Such a $Cu^{2+}$ ion-induced thickness change can be readily captured by the reflective spectrum with a spectrometer.

We chose poly(acrylamide-co-acrylic-acid-co-N-allylacrylamide) (poly(AAm-co-AAc-co-AAene)) as the hydrogel network with imidazole ligands covalently linked to it. A thin film of the hydrogel was fabricated via *in-situ* photo-polymerization during spin-coating on a Si wafer as the reflective substrate (Figure S5, Supporting Information). Considering a hydrated hydrogel has almost identical refractive index to the aqueous solution of analyte, a nanometer-thin layer of gold (Au) was subsequently sputtered on the hydrogel surface, for the purpose of enhancing the reflectivity at the aqueous solution-gel interface

for optimal interference, while ensuring good optical transparency and liquid permeability. When a droplet of $Cu^{2+}$ aqueous solution is applied on the surface of the hydrogel film with gold coating, clear and sharp peaks in the spectrum appears, indicating the effective improvement of interference compared to the hydrogel film without gold coating (**Figure 2**a). Such simple design with gold modification is proven to effectively produce a high signal-to-noise ratio in the optical sensing, allowing for the detection of liquidus analytes (Figure S5, Supporting Information). Importantly, this successfully expands the use cases of the platform to accommodate all forms of analytes.[11]

As the hydrogel film is covalently bonded to the Si wafer substrate during the in situ polymerization, the swelling of the hydrogel induces the thickness increase of the film. The film is washed, dried and swelled to a same initial thickness before applying different analyte solutions for multiple cycles of sensing tests. The thicknesses of the film before and after applying the analyte were measured by the reflective spectrum with an optical spectrometer under an illumination normal to the hydrogel surface. The thickness of the swollen hydrogel $d$ was calculated using Bragg's Law, $2nd = m\lambda$, where $n$ is the refractive index of the hydrogel, $m$ is a known integer, and $\lambda$ is the wavelength of the incident wave (detailed information, see Supporting Information).

Figure 2b shows the complete reflective spectra for the $Cu^{2+}$-specific hydrogel sensing a droplet of 10 µL with different concentrations of $Cu^{2+}$. Each curve exhibits three peaks around 458.7, 533.6, and 639.8 nm. These peaks shift toward shorter wavelength as the concentration of $Cu^{2+}$ increases. Taking the 639.8 nm peak as an example (Figure 2c), the peak shifts from 639.8 to 589.1 nm with different concentrations of $Cu^{2+}$.
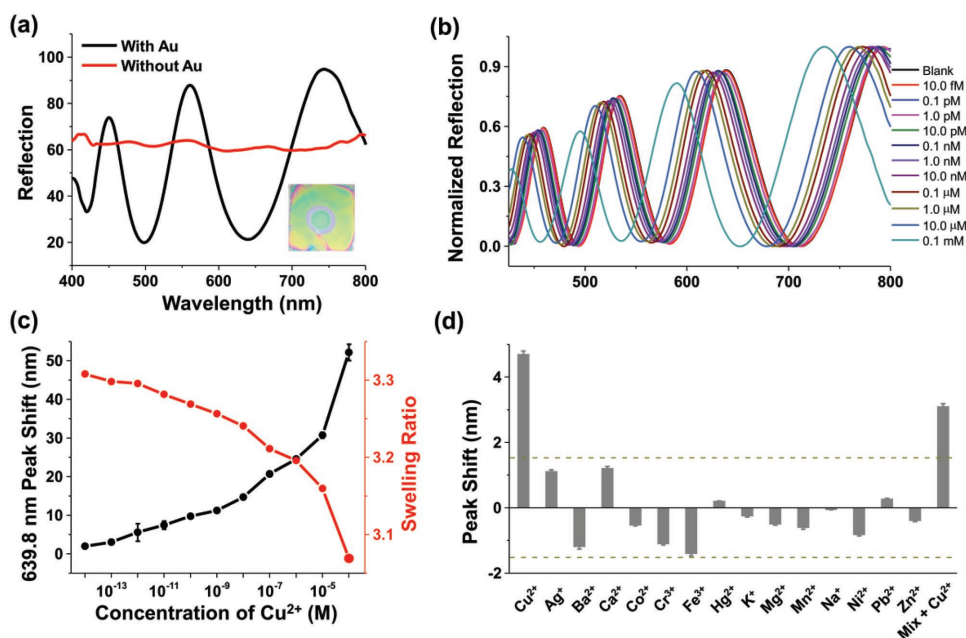


**Figure 2.** High sensitivity and selectivity of the $Cu^{2+}$ sensor. a) Reflective spectra of the $Cu^{2+}$ sensor with and without the sputtered gold film on the surface. b) The complete reflective spectra of the sensor with different concentrations of $Cu^{2+}$. The curves for blank solution and 10.0 fM overlap due to the small peak shift. c) The reflective peak shift and the swelling ratio measured as a function of the concentration of $Cu^{2+}$ at the wavelength of 639.8 nm. d) Reflective peak shifts at 458.7 nm induced by $Cu^{2+}$ of $10^{-11}$ M and 14 different metal ions of $10^{-9}$ M, as well as a mixture of them. The dash lines represent the resolution of the spectrometer (1.5 nm). All error bars indicate the standard deviation of three parallel experiments.

Considering the resolution of the optical spectrometer used here is 1.5 nm, only a peak shift above this resolution is considered as an effective sensing signal. Based on this, we achieved a wide detecting range of $Cu^{2+}$ concentration from $10^{-14}$ to $10^{-4}$ M. When a drop of $10^{-14}$ M $Cu^{2+}$ was applied on the film, the peak blue-shifted by 2.3 nm, still above the resolution of 1.5 nm. According to the curve in Figure 2c, the lowest concentration we can detect is about $1.3 \times 10^{-15}$ M $Cu^{2+}$, mainly limited by the resolution of the spectrometer used in this study (1.5 nm). Without such instrument limit, theoretically such a sensing principle could allow the lowest LOD to reach $2.2 \times 10^{-17}$ M on such a simple hydrogel thin-film system. The low LODs of our sensor is thus far below the maximum tolerable concentration of $Cu^{2+}$ in the standard drinking water ($2 \times 10^{-5}$ M) established by the U.S. Environmental Protection Agency.[8b] The thickness of the swollen hydrogel film under each $Cu^{2+}$ concentration was then calculated accordingly from the peak shift. The swelling ratio of the film was characterized as the ratio between the thickness of the swollen hydrogel and that of the dry gel (Figure 2c). The swelling ratio decreases from 3.31 to 3.07 as the concentration changes from $10^{-14}$ to $10^{-4}$ M, which confirms the effective additional crosslinks of hydrogel generated by the $Cu^{2+}$-ligand complex.

We further enhanced the reliability of the detection by reading the shifts of all the three peaks. We chose four different concentrations of $Cu^{2+}$ and all the three corresponding peak shifts (Figure S11, Supporting Information). The peak shifts are all higher than the resolution (1.5 nm) for $Cu^{2+}$ concentration as low as $1.0 \times 10^{-12}$ M. The ultralow detecting limit is again confirmed for our sensor. With our rationally selected hydrogel thickness, multiple peaks can be obtained in one sensor at once, serving as a built-in sensor array and leading to more reliable sensing results.

Next, we verified the specificity of the $Cu^{2+}$ sensor against other 14 interfering metal ions, including $Ag^+$, $Ba^{2+}$, $Ca^{2+}$, $Co^{2+}$, $Cr^{3+}$, $Fe^{3+}$, $Hg^{2+}$, $K^+$, $Mg^{2+}$, $Mn^{2+}$, $Na^+$, $Ni^{2+}$, $Pb^{2+}$, and $Zn^{2+}$. We tested it by applying a mixture solution of all the 15 ions, which contains $1.0 \times 10^{-11}$ M $Cu^{2+}$ and other ions of $1.0 \times 10^{-9}$ M (two orders of magnitude higher than $Cu^{2+}$ concentration). By high contrast, the peak shifts induced by all the other ions are significantly below the detection limit of the spectrometer and much smaller than the peak shift induced by $Cu^{2+}$ (4.7 nm) (Figure 2d). This suggests a high selectivity of our sensor in identifying $Cu^{2+}$, with great potential for real-life applications with various water or biofluid sources. The sensor can be recovered by being rinsed with or immersed in an acid solution.[15]

The experimentally observed high selectivity and sensitivity of the sensor can be explained by its chemical-mechanical-optical signal transducing process. The binding constant between the ligand and $Cu^{2+}$ (log $K_a$ = 12.6) is much higher than those between the ligand and other metal ions (Table S1, Supporting Information).[14,16] The high selectivity of the sensor toward $Cu^{2+}$ essentially originates from such a strong binding. Furthermore, we hypothesize that the high sensitivity is due to the localized concentration in the hydrogel, described as following. The total amount of ligands in the hydrogel is $10^{-8}$ mole, measured by X-ray photoelectron spectroscopy (Figure S10, Supporting Information). Considering the planar length and width

of the hydrogel film is 1.0 cm, and the thickness is on the order of 1 μm, the average concentration of ligands in the hydrogel matrix is about 0.77 M in the fully swollen hydrogel. For comparison, the concentration of $Cu^{2+}$ in the 10 μL analyte droplet ranges from $10^{-14}$ to $10^{-4}$ M. Because of the much higher ligand concentration together with the strong ion-ligand binding, as soon as the 10 μL (i.e., $10^{10}$ μm³) $Cu^{2+}$ solution is applied on the hydrogel film, the $Cu^{2+}$ will be locally confined within a much smaller volume of the hydrogel and thus be significantly concentrated. This concentrated $Cu^{2+}$ then causes a detectable thickness change of the hydrogel using the spectrometer, even when the initial concentration in the sensing droplet is as small as $10^{-14}$ M.

To verify this hypothesis that the majority of $Cu^{2+}$ ions were concentrated locally near the area where the drop was applied, we fabricated the same hydrogel sensor with two gold spots on its surface. As shown in **Figure 3**a, the two spots with 5.0 mm apart from each other were located on the same hydrogel film. After adding 10 μL of $Cu^{2+}$ at $10^{-11}$ M at Spot 1, we recorded both the spectra at the two spots. We observed an evident peak shift at Spot 1 (Figure 3b), but no shift at Spot 2 (Figure 3c). This proves that almost all the $Cu^{2+}$ ions have been effectively absorbed by the hydrogel at Spot 1 and formed complexes locally, without diffusing and reaching to the hydrogel at Spot 2. This experimentally revealed the diffusion length and the effective sensing area for 10 μL analyte of $10^{-11}$ M $Cu^{2+}$ is no more than 5.0 mm, which is the minimum distance that we can set the two sensing spots apart in our experimental condition.

To further estimate the more accurate approximate size of the hydrogel area where $Cu^{2+}$ ions are mostly concentrated, we adopt the theory of hydrogel swelling (see the Supporting Information for the detailed calculation).[17] We assume that after diffusion and binding, the $Cu^{2+}$ is homogeneously distributed throughout the thickness of the hydrogel, and within a circular area surrounding the location where the drop has been applied. We call this area the effective area of binding for the sensor. Outside the effective area, we assume there is no $Cu^{2+}$. The diameter of the estimated effective area is 1.44 μm for initially $10^{-14}$ M of $Cu^{2+}$, and 94.2 μm for initially $10^{-9}$ M of $Cu^{2+}$ (Figure 3d). The local concentration of $Cu^{2+}$ in the effective area in the hydrogel is further estimated to reach as high as nearly $10^9$ times of the original concentration in the droplet of $Cu^{2+}$ solution (Figure 3d). This large effect of localization enhances the signal transduction from the chemical binding to the optical spectrum, by increasing the change of the hydrogel swelling ratio at the local detecting spot.

The effect of binding localization also provides advantage of small detecting size of our sensor. The minimum size required for the hydrogel sensor to detect the 10 μL solution can be estimated by the effective binding area. For example, to detect the $Cu^{2+}$ concentration of $10^{-14}$ M, a sensor of only 1.44 μm diameter is needed. The current hydrogel sensor has the potential to be further fabricated with smaller size but same sensitivity and selectivity.

In addition to the high selectivity and sensitivity, the sub-micrometer film thickness and the optical detection ensure the fast response of our sensor. The binding between the ligands and $Cu^{2+}$ takes only a few minutes.[18] The diffusivity of ions and water molecules in a hydrogel
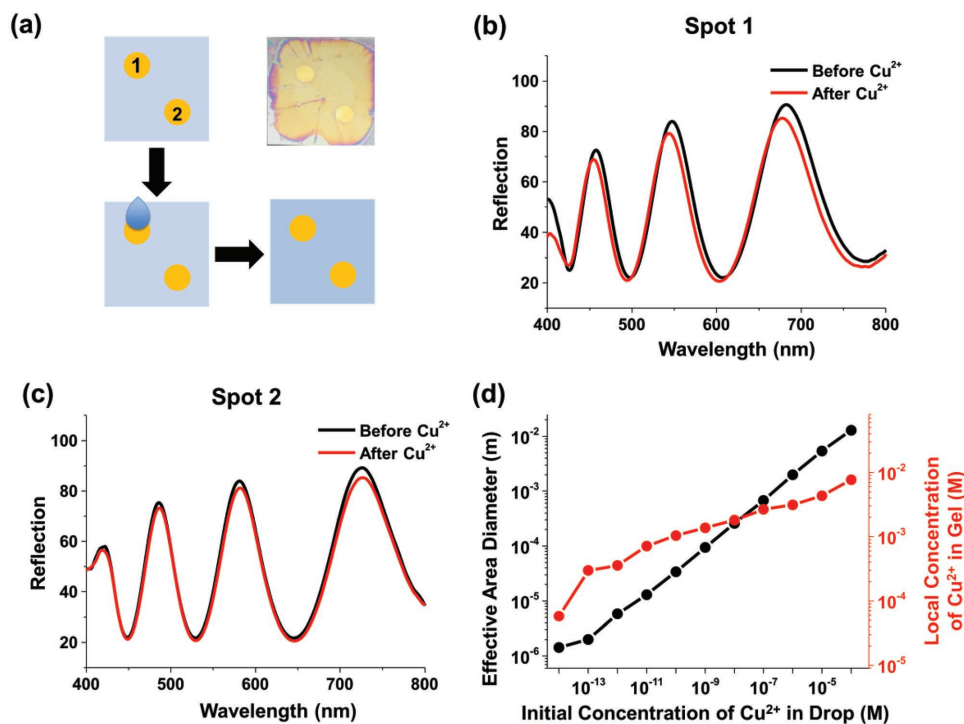
ADVANCED
SCIENCE NEWS
www.advancedsciencenews.com

ADVANCED
MATERIALS
www.advmat.de

**Figure 3.** The localized binding of $Cu^{2+}$ in the sensor and small effective area. a) The experimental setup for verifying the localized binding. The distance between Spot 1 and Spot 2 is about 5.0 mm. b,c) The reflective spectra before and after applying 10 μL of $Cu^{2+}$ with $10^{-11}$ M is recorded as in Spot 1 (b) and Spot 2 (c). d) The estimated diameter of the effective area of binding and the local concentration of $Cu^{2+}$ within the effective area.

is approximately $D \approx 10^{-10}$ m$^2$ s$^{-1}$.[19] Taking the thickness of the hydrogel as $h \approx 800$ nm, we estimate the time scale of the diffusion is $h^2/D \approx 0.01$ s. As a result, the whole sensing process takes a few minutes, limited by the reaction of binding. The response of the sensor is at least as fast as other current sensing methods for $Cu^{2+}$.[5b,16,20]

Owing to the broad chemistry, robust physics, and modular design of the hydrogel interferometer, this universal chemical-mechanical-optical platform can be readily customized to sense a broad range of molecules. Here we demonstrate its capability of sensing biological macromolecules, such as proteins, by simply linking specific functional ligands to the polymer chains of the hydrogel. Specifically, the hydrogel functionalized with phenylboronic acid (PBA) as the ligand can sense glycoproteins peroxidase from horseradish (HRP) (**Figure 4**a). The PBA ligands can bind diols in the glycoprotein, forming a 1:1 complex.[21] The increase of anionic boronate species in the hydrogel upon binding with glycoproteins leads to hydrogel swelling, due to electrostatic force and osmotic pressure of ions.[22] The gel film swelling redshifts the reflection wavelength. The measured LOD of the glycoprotein sensor is about $10^{-11}$ mg mL$^{-1}$ (Figure 4b), with great selectivity over seven interfering proteins (Figure 4c).

The hydrogel sensor can also be fabricated on various substrates, such as glass, poly(ethylene terephthalate) (PET) and poly(dimethylsiloxane) (PDMS). These optically transparent substrates provide versatility of projecting and detecting optical signals from arbitrary sides of the sensor. To achieve this, we coated thin layers of gold on top of the hydrogel film, as well as between the film and the substrate (Figure 4d). With glass as the

substrate, the sensor showed a slight golden color induced by interference, but still highly transparent (Figure 4e). We tested the transparent sensor by choosing different combinations of the projecting–detecting optical signals, including directions of top–top, top–bottom, bottom–bottom and bottom–top. Evident peak shifts were observed in all cases, indicating effective sensing of the analyte. This omni-directional sensing broadens the flexibility in applying the hydrogel interferometer platform on various usage scenarios, such as detecting chemicals in a box or room from outside, without entering the enclosed environment, and wearable sweat sensor which biocompatible and soft like tissue hydrogels can adhere on the human skins directly to avoid the uncomfortable feelings caused by the hard electronic devices and show the sensing signals on the opposite directions after absorbing the sweats.[23]

Flexible and stretchable sensors for wearable devices, such as human-wearable sensors for health monitoring[24] and feedback sensors in soft robots,[9b,25] have been actively developed. The transparent sensor demonstrated here can also be made flexible and stretchable using PET or PDMS as the substrates. All materials including hydrogels can be susceptible to fatigue under cyclic loads.[26] To preliminarily test the resistance to fatigue of the stretchable sensor, we bent or stretched the hydrogel-PET/PDMS sensor for 200 cycles, and measured the reflective spectrum of the hydrogel film. After 200 cycles, the reflective spectrum remained nearly the same as what was measured before the cyclic bending or stretching (Figure 4g,h). No obvious crack or flaw was observed on the surface of the hydrogel (Figures S16 and S17, Supporting Information). With the same concentration of $Cu^{2+}$ applied, the peak shift

**ADVANCED
SCIENCE NEWS**
www.advancedsciencenews.com

**ADVANCED
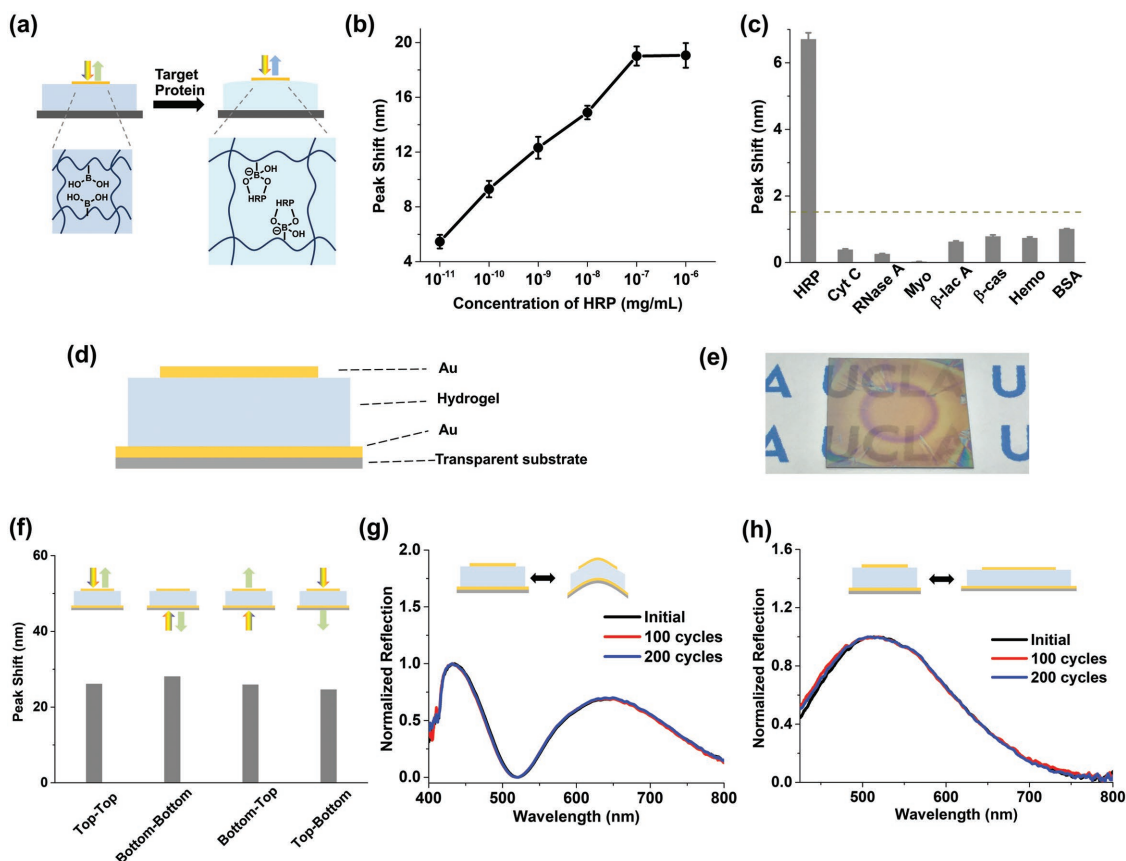MATERIALS**
www.advmat.de

**Figure 4.** Generality of the sensing platform. a) The detection mechanism of the glycoprotein-specific sensor. b) Reflective peak shift at the wavelength of 601.0 nm as a function of the concentration of HRP (from $10^{-11}$ to $10^{-6}$ mg mL$^{-1}$). c) Reflection peak shifts at the wavelength of 452.0 nm of $10^{-10}$ mg mL$^{-1}$ HRP compared to $10^{-8}$ mg mL$^{-1}$ of seven other different proteins. The dash line represents the resolution of the spectrometer (1.5 nm). d) The configuration of the hydrogel sensor on transparent substrates. e) The photo of the hydrogel sensor on glass substrate. f) Reflective peak shifts of the hydrogel sensor on glass substrate induced by Cu$^{2+}$ from different projecting–detecting directions including top–top, bottom–bottom, bottom–top, and top–bottom. g) Reflective spectra of the hydrogel sensor on PET substrate before and after cycles of bending. h) Reflective spectra of the hydrogel sensor on PDMS substrate before and after cycles of stretching. All error bars indicate the standard deviation of three parallel experiments.

of the sensor kept the same before and after the cyclic test. As a stretchable sensor, the effect of mechanical stretch on the hydrogel film thickness change can be decoupled from the effect of analyte by individually measuring the peak shift during stretch without Cu$^{2+}$. The reflective peak shifted by about 100 nm when the tensile strain was 50% (Figure S17, Supporting Information). Being integrated in parallel as an array, the stretchable sensors are capable of sensing both metal ions and mechanical deformation.

The general sensing platform based on hydrogel interferometer that exhibits remarkable high performance takes advantage of coupling two attributes: optical interference and responsive hydrogels. Optical interference has been serving as a powerful tool in detecting small change of length on the order of nm.[27] The optical interference-based detecting technique has even been pushed beyond its limit to successfully measure a distance change of $10^{-4}$ times of the width of a proton ($10^{-19}$ m) by the Laser Interferometer Gravitational-wave Observatory.[28] The spectrum of thin-film interference changes with the film thickness is also commonly seen in daily life, just like the various iridescent colors

induced by the nonuniform thickness of a soap bubble or oil-covered water.[29] Responsive hydrogels are capable of large deformation triggered by external stimuli such as solvent,[30] pH,[22,31] temperature[32] and humidity.[11,33] Hydrogel as a cross-linked hydrophilic polymer network is known as super-absorbent.[34] The dehydrated hydrogel with ligands incorporated can facilitate the absorption of a large amount of analyte in aqueous solution within very small volume, which spontaneously localizes and concentrates the analyte concentration. Overall, the local concentrating effect, multiplied by the signal amplification effect, enables the ultrahigh sensitivity of this hydrogel interferometer-based sensor. In addition, a hydrogel can be functionalized to become responsive to different environmental cues, by linking specific functional groups or monomers to its polymer chains, which provides an analyte-specific matrix. In most cases, the time scale of response is governed by diffusion, which decreases quadratically with the feature size of the hydrogel.[35] The 0.1–1 µm scale thickness of our hydrogel film enables 10–100 second-scale fast response for real-time sensing. The cost of fabricating sub-micrometer hydrogels and testing various analytes is low, as they require

**ADVANCED
SCIENCE NEWS**

www.advancedsciencenews.com

**ADVANCED
MATERIALS**

www.advmat.de

only small quantities of materials.[36] The hydrogel can be biocompatible with good stretchability, making it a suitable material for wearable sensor.[37] These advantages together make the responsive hydrogel an ideal material for fabricating high-performance sensing systems,[38] and being integrated with optical interference.

In summary, we report a universal physical principle based on hydrogel interferometry sensor that can effectively enhance the chemical detection sensitivity for several orders of magnitude (i.e., $10^2$–$10^4$), by remarkable local concentrating effect ($10^9$ times) and large signal amplification in a chemo-mechano-optical signal transduction. Specifically, the strong analyte binding with the large amount of ligands carried on the shrinkable porous gel matrix produces unique local concentrating effect for $10^9$ times, makes extremely low concentrated molecules detectable, avoiding preconcentrating or multistep processes. Meanwhile, the specific chemical reaction between the selected ligand and the target analyte gives the platform high selectivity. Here the demonstrated picoM-femtoM high sensitivity ($10^{-13}$–$10^{-15}$ M) in metal ion detection against 14 interfering ions, as well as protein detection. These showcase the promising potential in on-site analysis and even real-time monitoring of seawater or wastewater and in new point-of-care or health monitoring technologies, without the needs of complex procedures and costly large equipment required by current methods. Device-wise, its micrometer scale effective sensing area, optical transparency, and mechanical flexibility (robustness over cycles of bending or stretching) compatible with different substrates show great potential as micro-scale wearable sensors and easy integration. Overall, this simple and general design principle is applicable to almost any porous soft materials, providing a practical solution to enhancing the performance of many sensors of different sensing mechanisms with different responses to not only various chemicals but also temperature, mechanical and other physical environmental cues. It is hoped that this platform will open the avenues to new development of sensors with high performance, low cost, and easy fabrication for health and environmental real-time monitoring.

## Supporting Information

Supporting Information is available from the Wiley Online Library or from the author.

## Conflict of Interest

The authors declare no conflict of interest.

[1] T. M. Swager, *Angew. Chem., Int. Ed.* **2018**, *57*, 4248.

[2] a) S. Bai, C. Sun, H. Yan, X. Sun, H. Zhang, L. Luo, X. Lei, P. Wan, X. Chen, *Small* **2015**, *11*, 5807; b) S. Yang, L. Liu, W. Chen, W. Jin, J. Zhou, H. Zhang, G. S. Zakharova, *Sens. Actuators, B* **2016**, *226*, 478; c) T. Wang, Y. Guo, P. Wan, H. Zhang, X. Chen, X. Sun, *Small* **2016**, *12*, 3748.

[3] a) S. Takano, M. Tanimizu, T. Hirata, Y. Sohrin, *Nat. Commun.* **2014**, *5*, 5663; b) A. L. Campbell, S. Mangan, R. P. Ellis, C. Lewis, *Environ. Sci. Technol.* **2014**, *48*, 9745; c) J. M. Lee, E. A. Boyle, Y. Echegoyen-Sanz, J. N. Fitzsimmons, R. Zhang, R. A. Kayser, *Anal. Chim. Acta* **2011**, *686*, 93; d) K. H. Coale, K. W. Burland, *Limnol. Oceanogr.* **1988**, *33*, 1084.

[4] A. Ala, A. P. Walker, K. Ashkan, J. S. Dooley, M. L. Schilsky, *Lancet* **2007**, *369*, 397.

[5] a) Brief Guide to Analytical Methods for Measuring Lead in Blood. World Health Organization, **2011**; b) C. Hazra, S. Ullah, L. G. Caetano, S. J. L. Ribeiro, *J. Mater. Chem. C* **2018**, *6*, 153.

[6] W. Zheng, H. Li, W. Chen, J. Zhang, N. Wang, X. Guo, X. Jiang, *Small* **2018**, *14*, 1703857.

[7] a) F. Watzinger, K. Ebner, T. Lion, *Mol. Aspects Med.* **2006**, *27*, 254; b) A. Ymeti, J. Greve, P. V. Lambeck, T. Wink, S. W. van Hovell, T. A. Beumer, R. R. Wijn, R. G. Heideman, V. Subramaniam, J. S. Kanger, *Nano Lett.* **2007**, *7*, 394.

[8] a) J. Wang, H. Chen, F. Ru, Z. Zhang, X. Mao, D. Shan, J. Chen, X. Lu, *Chem. – Eur. J.* **2018**, *24*, 3499; b) S. Wang, C. Liu, G. Li, Y. Sheng, Y. Sun, H. Rui, J. Zhang, J. Xu, D. Jiang, *ACS Sens.* **2017**, *2*, 364; c) T. Liu, Y. Q. Luo, L. Y. Kong, J. M. Zhu, W. Wang, L. Tan, *Sens. Actuators, B* **2016**, *235*, 568; d) H. Ouyang, Q. Shu, W. Wang, Z. Wang, S. Yang, L. Wang, Z. Fu, *Biosens. Bioelectron.* **2016**, *85*, 157; e) R. Hu, T. Furukawa, X. Wang, M. Nagatsu, *Adv. Funct. Mater.* **2017**, *27*, 1702232; f) A. K. Yetisen, Y. Montelongo, M. M. Qasim, H. Butt, T. D. Wilkinson, M. J. Monteiro, S. H. Yun, *Anal. Chem.* **2015**, *87*, 5101.

[9] a) J. Ye, Y. Chen, Z. Liu, *Angew. Chem., Int. Ed.* **2014**, *53*, 10386; b) Y. J. Liu, W. T. Cao, M. G. Ma, P. Wan, *ACS Appl. Mater. Interfaces* **2017**, *9*, 25559; c) H. Y. Peng, Y. Jiao, X. Xiao, B. B. Chen, M. He, Z. R. Liu, X. Zhang, B. Hu, *J. Anal. At. Spectrom.* **2014**, *29*, 1112; d) C. H. Lu, Y. Zhang, S. F. Tang, Z. B. Fang, H. H. Yang, X. Chen, G. N. Chen, *Biosens. Bioelectron.* **2012**, *31*, 439.

[10] a) J. A. Cotruvo Jr., A. T. Aron, K. M. Ramos-Torres, C. J. Chang, *Chem. Soc. Rev.* **2015**, *44*, 4400; b) K. P. Carter, A. M. Young, A. E. Palmer, *Chem. Rev.* **2014**, *114*, 4564; c) T. Hirayama, G. C. Van de Bittner, L. W. Gray, S. Lutsenko, C. J. Chang, *Proc. Natl. Acad. Sci. USA* **2012**, *109*, 2228; d) L. Xi, L. Zheng, Y. Ying-Wei, *Adv. Mater.* **2018**, *30*, 1800177.

[11] M. Qin, M. Sun, R. Bai, Y. Mao, X. Qian, D. Sikka, Y. Zhao, H. J. Qi, Z. Suo, X. He, *Adv. Mater.* **2018**, *30*, 1800468.

[12] a) L. Ionov, *Mater. Today* **2014**, *17*, 494; b) X. He, M. Aizenberg, O. Kuksenok, L. D. Zarzar, A. Shastri, A. C. Balazs, J. Aizenberg, *Nature* **2012**, *487*, 214; c) A. Shastri, L. M. McGregor, Y. Liu, V. Harris, H. Nan, M. Mujica, Y. Vasquez, A. Bhattacharya, Y. Ma, M. Aizenberg, O. Kuksenok, A. C. Balazs, J. Aizenberg, X. He, *Nat. Chem.* **2015**, *7*, 447; d) Z. Zhao, N. Hamdan, L. Shen, H. Nan, A. Almajed, E. Kavazanjian, X. He, *Environ. Sci. Technol.* **2016**, *50*, 12401.

[13] X. Lin, Y. Hong, C. Zhang, R. Huang, C. Wang, W. Lin, *Chem. Commun.* **2015**, *51*, 16996.

**ADVANCED
SCIENCE NEWS**

www.advancedsciencenews.com

**ADVANCED
MATERIALS**

www.advmat.de

[14] R. J. Sundberg, R. B. Martin, *Chem. Rev.* **1974**, *74*, 471.

[15] B. L. Rivas, H. A. Maturana, M. J. Molina, M. R. Gomez-Anton, I. F. Pierola, *J. Appl. Polym. Sci.* **1998**, *67*, 1109.

[16] W. Hong, W. H. Li, X. B. Hu, B. Y. Zhao, F. Zhang, D. Zhang, *J. Mater. Chem.* **2011**, *21*, 17193.

[17] a) W. Hong, Z. S. Liu, Z. G. Suo, *Int. J. Solids Struct.* **2009**, *46*, 3282; b) S. Cai, Z. G. Suo, *EPL* **2012**, *97*, 34009.

[18] T. Cam, B. Osman, A. Kara, E. Demirbel, N. Besirli, G. Irez, *J. Appl. Polym. Sci.* **2014**, *131*, http://doi.org/10.1002/app.39751.

[19] J. Y. Li, Y. H. Hu, J. J. Vlassak, Z. G. Suo, *Soft Matter* **2012**, *8*, 8121.

[20] R. Wu, S. Zhang, J. Lyu, F. Lu, X. Yue, J. Lv, *Chem. Commun.* **2015**, *51*, 8078.

[21] C. Zhang, M. D. Losego, P. V. Braun, *Chem. Mater.* **2013**, *25*, 3239.

[22] R. Marcombe, S. Q. Cai, W. Hong, X. H. Zhao, Y. Lapusta, Z. G. Suo, *Soft Matter* **2010**, *6*, 784.

[23] a) L. C. Tai, W. Gao, M. H. Chao, M. Bariya, Q. P. Ngo, Z. Shahpar, H. Y. Y. Nyein, H. Park, J. Sun, Y. Jung, E. Wu, H. M. Fahad, D. H. Lien, H. Ota, G. Cho, A. Javey, *Adv. Mater.* **2018**, *30*, 1707442; b) C. C. Kim, H. H. Lee, K. H. Oh, J. Y. Sun, *Science* **2016**, *353*, 682.

[24] J. Y. Sun, C. Keplinger, G. M. Whitesides, Z. Suo, *Adv. Mater.* **2014**, *26*, 7608.

[25] K. Tian, J. Bae, S. E. Bakarich, C. Yang, R. D. Gately, G. M. Spinks, M. In Het Panhuis, Z. Suo, J. J. Vlassak, *Adv. Mater.* **2017**, *29*, 1604827.

[26] a) J. Tang, J. Li, J. J. Vlassak, Z. Suo, *Extreme Mech. Lett.* **2017**, *10*, 24; b) R. B. Bai, Q. S. Yang, J. D. Tang, X. P. Morelle, J. Vlassak, Z. G. Suo, *Extreme Mech. Lett.* **2017**, *15*, 91; c) R. B. Bai, J. W. Yang, X. P. Morelle, C. H. Yang, Z. G. Suo, *ACS Macro Lett.* **2018**, *7*, 312.

[27] Q. M. Zhang, W. Xu, M. J. Serpe, *Angew. Chem., Int. Ed.* **2014**, *53*, 4827.

[28] https://www.ligo.caltech.edu/

[29] L. He, M. Janner, Q. Lu, M. Wang, H. Ma, Y. Yin, *Adv. Mater.* **2015**, *27*, 86.

[30] Q. Lin, X. Hou, C. Ke, *Angew. Chem., Int. Ed.* **2017**, *56*, 4452.

[31] L. A. Sharpe, J. E. Vela Ramirez, O. M. Haddadin, K. A. Ross, B. Narasimhan, N. A. Peppas, *Biomacromolecules* **2018**, *19*, 793.

[32] a) Z. X. Zhang, K. L. Liu, J. Li, *Angew. Chem., Int. Ed.* **2013**, *52*, 6180; b) J. H. Liu, G. S. Chen, M. Y. Guo, M. Jiang, *Macromolecules* **2010**, *43*, 8086; c) E. Sato Matsuo, T. Tanaka, *J. Chem. Phys.* **1988**, *89*, 1695.

[33] H. Li, S. Voci, V. Ravaine, N. Sojic, *J. Phys. Chem. Lett.* **2018**, *9*, 340.

[34] a) S. Pathan, S. Bose, *ACS Omega* **2018**, *3*, 5910; b) F. B. Xiao, Y. F. Sun, W. F. Du, W. H. Shi, Y. Wu, S. Z. Liao, Z. Y. Wu, R. Q. Yu, *Adv. Funct. Mater.* **2017**, *27*, 1702147; c) W. Li, J. Wang, J. Ren, X. Qu, *Adv. Mater.* **2013**, *25*, 6737.

[35] X. Zhang, Y. Guan, Y. Zhang, *Biomacromolecules* **2012**, *13*, 92.

[36] I. Tokarev, S. Minko, *Soft Matter* **2009**, *5*, 511.

[37] C. Yang, Z. Suo, *Nat. Rev. Mater.* **2018**, *3*, 125.

[38] a) M. R. Islam, Y. F. Gao, X. Li, M. J. Serpe, *J. Mater. Chem. B* **2014**, *2*, 2444; b) A. K. Yetisen, I. Naydenova, F. da Cruz Vasconcellos, J. Blyth, C. R. Lowe, *Chem. Rev.* **2014**, *114*, 10654; c) Z. Cai, A. Sasmal, X. Liu, S. A. Asher, *ACS Sens.* **2017**, *2*, 1474.